

Atomic model of a myosin filament in the relaxed state

John L. Woodhead^{1*}, Fa-Qing Zhao^{1*}, Roger Craig^{1*}, Edward H. Egelman², Lorenzo Alamo³ & Raúl Padrón³

Contraction of muscle involves the cyclic interaction of myosin heads on the thick filaments with actin subunits in the thin filaments¹. Muscles relax when this interaction is blocked by molecular switches on either or both filaments². Insight into the relaxed (switched OFF) structure of myosin has come from electron microscopic studies of smooth muscle myosin molecules, which are regulated by phosphorylation. These studies suggest that the OFF state is achieved by an asymmetric, intramolecular interaction between the actin-binding region of one head and the converter region of the other, switching both heads off³. Although this is a plausible model for relaxation based on isolated myosin molecules, it does not reveal whether this structure is present in native myosin filaments. Here we analyse the structure of a phosphorylation-regulated striated muscle thick filament using cryo-electron microscopy. Three-dimensional reconstruction and atomic fitting studies suggest that the ‘interacting-head’ structure is also present in the filament, and that it may underlie the relaxed state of thick filaments in both smooth and myosin-regulated striated muscles over a wide range of species.

The thick filaments of muscle are polymers of myosin II (reviewed in ref. 4). The α -helical coiled-coil myosin tails form the backbone of the filament, whereas the heads (two from each molecule) lie on the surface, where they can interact with actin. In the relaxed state, the myosin heads in most striated muscles are helically ordered^{5,6}. Electron microscopy (EM) and three-dimensional (3D) helical reconstruction of isolated filaments have produced models of head conformation and interactions in the relaxed state^{7–12}. However, none of these models has provided compelling insight into the structural basis of relaxation. Most have been based on negatively stained specimens, which can have staining and drying artefacts, and the resolution has been limited to ~ 5 nm, owing partly to limitations of the helical reconstruction technique. In this report we study a highly ordered species of thick filament (from tarantula striated muscle), use cryo-electron microscopy to preserve native structure, and carry out 3D reconstruction using a single particle approach. Fitting of the atomic structure of the myosin heads to the reconstruction provides key new insights into the molecular basis of relaxation.

Figure 1a shows a cryo-electron micrograph of purified thick filaments. The arrow-like structures, pointing towards the central bare-zone of the filament, represent the superposition of helically organized myosin heads on the top and bottom surfaces of the filament. Elongated substructure in the backbone, running parallel to the filament axis, is also apparent (Fig. 1b). An averaged 3D reconstruction of these filaments was computed by a real space, single particle technique that avoids important limitations of helical reconstruction (see Methods)¹³. The structure (~ 2.5 nm resolution) was similar in overall appearance to a 5 nm resolution helical reconstruction of negatively stained tarantula filaments^{7,8}, but

showed crucial new detail not seen previously (Fig. 1c; see also Supplementary Movie 1). The repeating motif on the surface of the filament, representing a pair of myosin heads, appears like a tilted ‘J’ (Fig. 1c, d). Four of these motifs, equally spaced around the filament circumference, form ‘crowns’ (Fig. 2a) that occur at regular axial intervals of 14.5 nm. This fourfold rotationally symmetric arrangement twists by 30° from one 14.5 nm level to the next, creating four parallel right-handed helical tracks, with a helical repeat of 43.5 nm (ref. 7). The structure thus repeats every third crown (Fig. 1c), with pairs of heads appearing at twelve equally spaced azimuthal positions in transverse view (Fig. 2b).

The backbone of the filament also reveals new detail. It is seen to comprise twelve approximately parallel strands, each ~ 4 nm in diameter (and therefore containing more than one 2 nm diameter myosin tail), centred at a radius of ~ 8 nm from the filament axis (Figs 1c and 2b). This is the first time that the structure of the backbone has been clearly seen in any thick filament reconstruction. The presence of such ‘subfilaments’ in the reconstruction is consistent with the backbone substructure seen in the raw images (Fig. 1b) and in earlier negative stain images⁷. Subfilaments of this size were proposed in a general model for the structure of the thick filament backbone based on X-ray diffraction of invertebrate muscles¹⁴. In this model it was suggested that each 4 nm-diameter subfilament contained three myosin tails in cross-section, and gave off a pair of myosin heads at every third level of myosin molecules. For filaments with the tarantula symmetry (fourfold rotational symmetry, helical repeat = 3×14.5 nm), the model predicts twelve subfilaments running parallel to the filament axis, exactly as we have observed. We also observe a narrow rod of density arising at each level of heads that has the correct size and orientation to be the subfragment-2 (S2) portion of the myosin tail connecting the two heads to the subfilament (Figs 2a, 3a and 4).

Interpretation of reconstructions is aided, and their effective resolution extended, by computationally ‘fitting’ atomic structures of the constituent subunits into the corresponding features in the reconstruction. The only available atomic model of a two-headed myosin is based on cryo-electron microscopy of two-dimensional crystals of vertebrate smooth muscle myosin^{3,15}. In the OFF state (in which the regulatory light chains are dephosphorylated), this myosin shows an asymmetric interaction between its two heads, with the actin-binding region of one head (the ‘blocked’ head) interacting with the converter and essential light chain regions of the other (the ‘free’ head). Simple visual inspection suggests that this asymmetric atomic structure fits into the J motif of the reconstruction (Fig. 1c, d). This is confirmed by 3D fitting of the motor domains and the light chain domains of the two heads as four independent rigid bodies (Fig. 3; see also Supplementary Movies 4, 5). An excellent fit to the density map is obtained that preserves the main characteristics of the

¹Department of Cell Biology, University of Massachusetts Medical School, Worcester, Massachusetts 01655, USA. ²Department of Biochemistry and Molecular Genetics, University of Virginia Health Sciences Center, Charlottesville, Virginia 22908, USA. ³Departamento de Biología Estructural, Instituto Venezolano de Investigaciones Científicas (IVIC), Caracas 1020A, Venezuela.

*These authors contributed equally to this work.

original atomic model, particularly with respect to the asymmetric motor domain interaction. There is a minor ($\sim 20^\circ$) difference in the angles that the light chain domains make with the motor domains (consistent with the known flexibility of the light chain domain/motor domain junction^{1,16}), but the spatial relationship of the light

chain domains to each other is essentially unchanged. Thus the head-head interaction previously observed in single molecules, and suggested to be the structural mechanism by which actomyosin ATPase is switched OFF³, is also a key feature of the relaxed native filament.

In addition to the volume filled by the two heads, a rod-like volume of density was observed running from the junction of the light chain domains at a shallow angle towards the filament shaft in the direction of the bare zone, eventually merging with the subfilament density (Figs 2a, 3a and 4). The size and positioning of this density suggest that it is the first portion of the myosin S2 tail emerging from the heads, and a 2 nm-diameter coiled-coil model of this part of S2 (ref. 3) is readily accommodated by the volume (Fig. 4a, b; see also Supplementary Movie 6). Thus the heads of the myosin molecule in the reconstruction are seen to be bent back towards the tail (Figs 1d, 3a, 4a and 5a, b). This 'bent-back' orientation has been shown to characterize the OFF-state of myosin molecules isolated from both vertebrate smooth^{17,18,19} and scallop striated muscle^{19,20}. Our fitting shows that this structure is also present in the filament. In addition, it reveals further intramolecular interactions that may contribute to the relaxed state of the filament. S2 lies close to the actin-binding interface of the blocked head (Fig. 5a, c; see also Supplementary Movie 5), consistent with the location of the myosin tail in isolated molecules in the OFF-state¹⁸. This interaction may help to keep the blocked head from interacting with actin in relaxed muscle. Our model may therefore explain both the necessity of a minimal

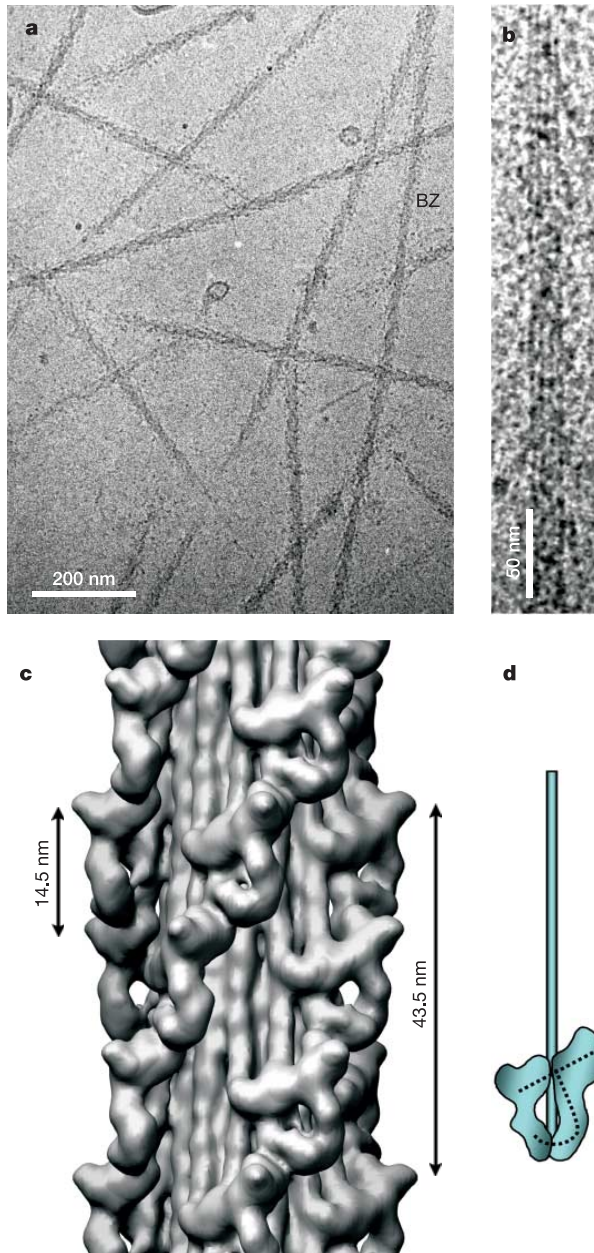


Figure 1 | Cryo-electron micrographs and 3D reconstruction of purified tarantula thick filaments. **a**, Field of filaments showing arrowhead motifs, pointing towards the central 'bare zone' (BZ)—the region free of myosin heads, where filament polarity reverses. This image was taken at high ($4.6 \mu\text{m}$) defocus to enhance contrast. **b**, High magnification filament image showing backbone substructure parallel to the filament axis. **c**, Surface view of 3D reconstruction (bare zone at top; compare with Supplementary Fig. 1). The repeating motif, representing a pair of myosin heads, has the appearance of a tilted J (see **d**); a similar motif was seen, less clearly, in a helical reconstruction of negatively stained tarantula filaments³. The filament backbone, lying beneath the heads, consists of subfilaments spaced ~ 4 nm apart and running parallel to the filament axis. **d**, Diagram showing interpretation of J motif in terms of a pair of interacting myosin heads³ bent towards the tail (heads and tail not to scale; tail truncated; compare with Fig. 5b).

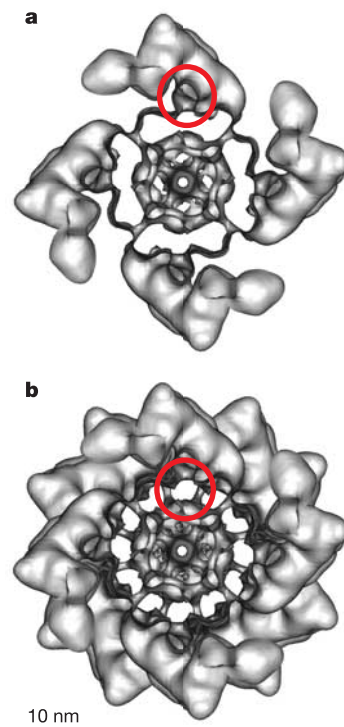


Figure 2 | Surface rendition of thick filament reconstruction looking along the filament axis from the bare zone. **a**, Single 14.5 nm repeat containing portions of two crowns of myosin heads, revealing the fourfold symmetry of the myosin head arrangement. The red circle indicates a rod-like volume, tilting towards the filament backbone, of size and location consistent with the initial portion of S2 of the myosin tail (Fig. 4; see Supplementary Fig. 2, Movies 2 and 3). **b**, Full 43.5 nm repeat (containing three 14.5 nm repeats), illustrating the presence of twelve subfilaments in the backbone running parallel to the filament axis (compare with Supplementary Fig. 3). Each subfilament (red circle), ~ 4 nm in diameter and centred ~ 8 nm from the filament axis, appears to be continuous through a full repeat. The material at lower radius in the filament core is of low density, possibly representing small amounts of nonmyosin proteins (Supplementary Fig. 3).

length of S2 for regulation²¹ and the importance of the actin-binding domain in the regulatory mechanism²².

The model also reveals possible intermolecular interactions between myosin molecules in different crowns, which can occur in the filament but not in single molecules. The converter and SH3 (src homology 3) regions of the blocked head lie close to the S2 arising from the next pair of heads away from the bare zone (Fig. 5b, c). The converter domain has been reported to be necessary for regulation²³. The essential light chain from the blocked head lies over the actin

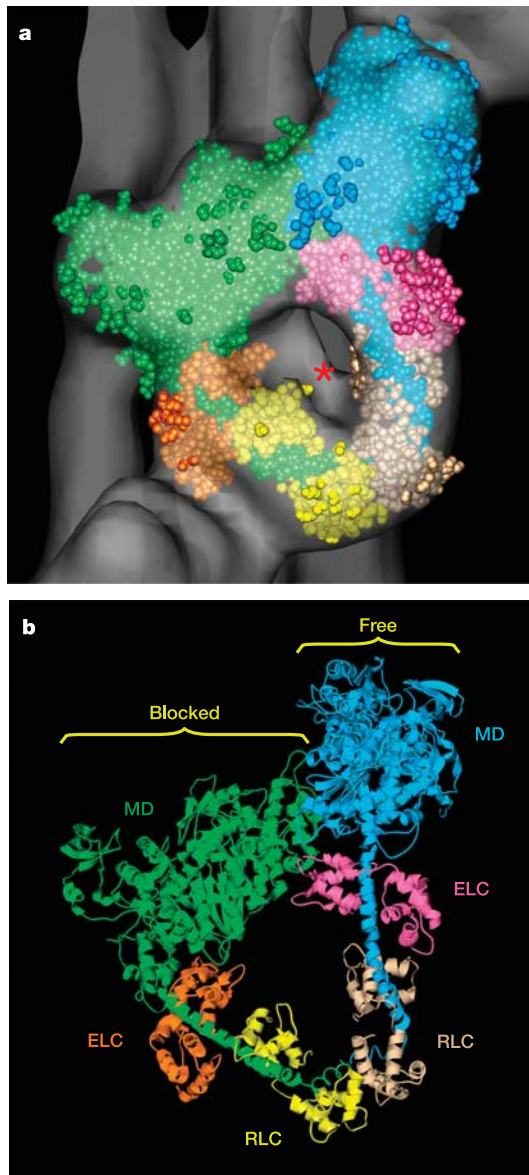


Figure 3 | Fitting of heads of smooth muscle HMM atomic model (PDB 1i84, ref. 3) to the tarantula thick filament 3D reconstruction. a, Best fit of atomic structure (space filling model) to the reconstruction (translucent envelope). The red asterisk shows a rod-like volume of density interpreted as S2 (see Fig. 4). **b**, Ribbon representation of the atomic structure from **a** shown without the reconstruction. MD, ELC and RLC of the blocked and free heads represent the motor domains, essential light chains and regulatory light chains, respectively. Note: this 2.5 nm resolution reconstruction gives an essentially unambiguous fit to the asymmetric HMM atomic structure. Previous 'splayed heads' structures were proposed before the HMM structure was available and were based on helical reconstruction of negatively stained filaments^{7,8} that lacked the resolution (5 nm) for an unambiguous fit.

binding domain of the free head from the axially adjacent molecule (Fig. 5b), which could limit interaction of the free head with actin.

The atomic thick filament model that we have proposed reconciles previous heavy meromyosin (HMM) crystal studies^{3,15}, single molecule EM observations^{17–20} and studies of regulation^{21–23}. In so doing, it suggests a compelling structural model for how phosphorylation-regulated myosin may be switched OFF in the filaments of resting muscle, and also how the filaments may be switched ON when muscle is activated. With this model, the relaxed heads of each myosin molecule lie close to the filament surface, interacting with each other, with S2 and with other myosin molecules. This would presumably inhibit both their interaction with actin (only 2–5 nm away) and their ATPase activity (see also ref. 3). On activation of muscle, Ca²⁺ is released into the cytosol, increasing thick filament

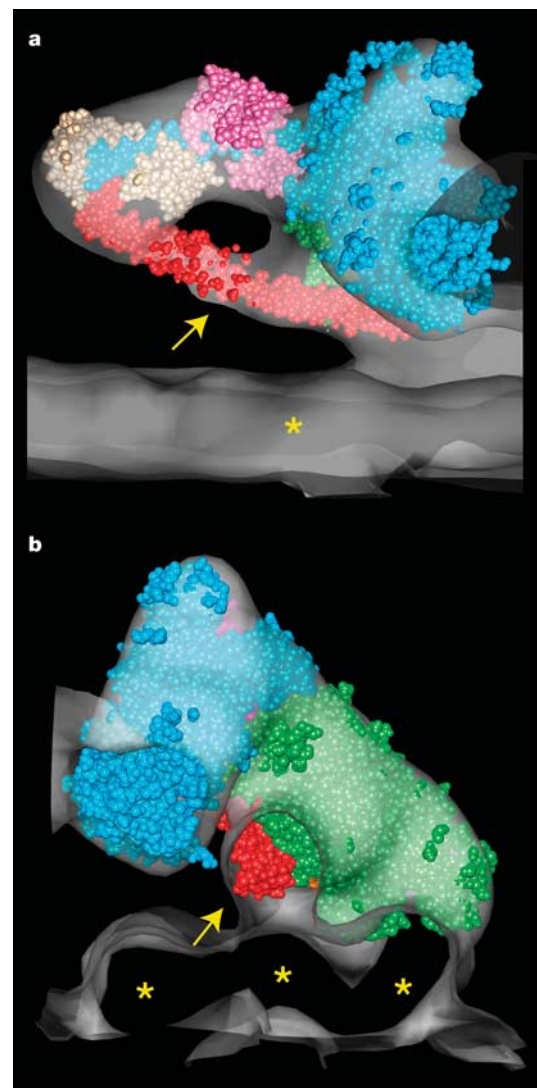


Figure 4 | Fitting of S2 into the reconstruction. a, b, Part of one J-motif and adjacent subfilaments (translucent envelope) are shown side-on (**a**), from the free head side (bare zone to the right) and end-on (**b**), from the bare zone (compare with top motif in Fig. 2a; see also Supplementary Movie 6). A rod-like volume (yellow arrows) slopes in the direction of the bare zone from the junction of the light chain domains towards the subfilaments (yellow asterisks) in the backbone. The amino-terminal part of S2, modelled as an α -helical coiled-coil³ (red space filling model), is readily accommodated by this volume. Note: for clarity, the blocked head (behind the free head) has been excluded from **a**.

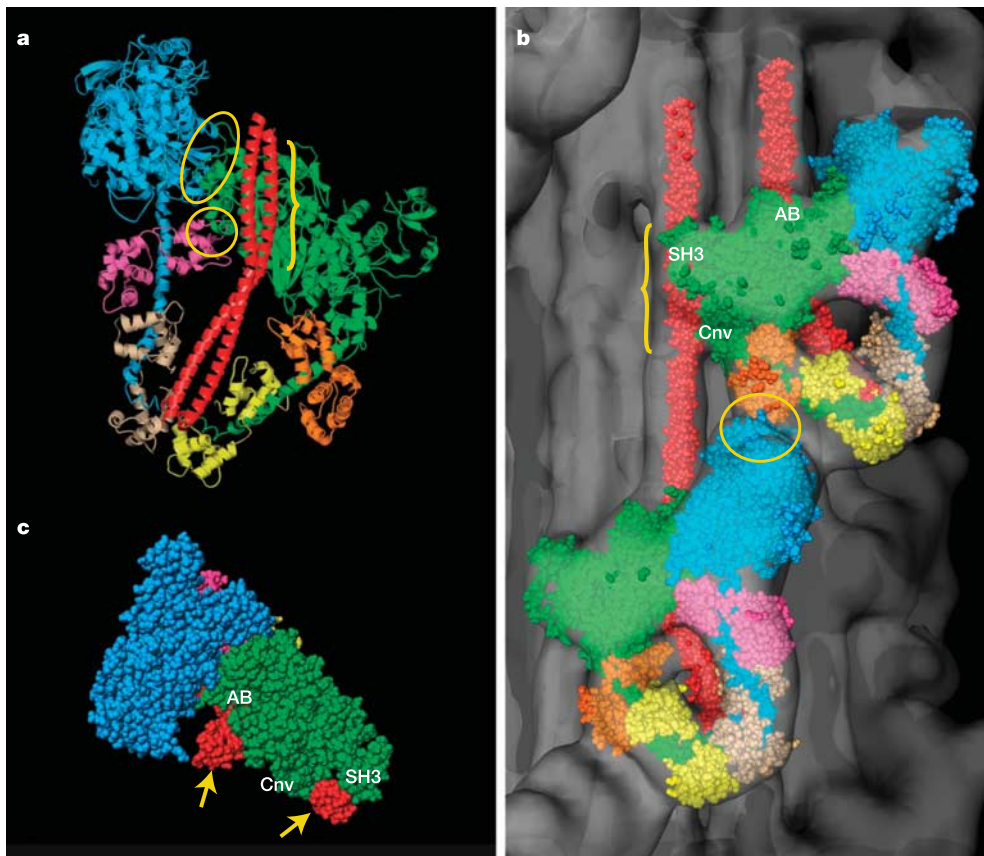


Figure 5 | Intramolecular and intermolecular interactions of myosin heads. **a**, Combined atomic models (ribbon representation) from Figs 3 and 4, including the two heads and two S2 'segments' (ref. 3), as viewed from the underlying subfilaments (compare with Supplementary Movie 5). Regions of possible intramolecular interactions include: the free motor domain and blocked motor domain (yellow ellipse); the blocked motor domain and free essential light chain (yellow circle); and the blocked motor domain and the S2 (yellow bracket). **b**, Surface representation of the reconstruction showing atomic models of HMM fitted into motifs from successive crowns. The S2 from the lower pair of heads has been extended towards the bare zone to fill a longer portion of the volume in this region. Possible intermolecular interactions are shown between the blocked essential light chain and the free motor domain (yellow ellipse), and the blocked motor domain and S2 (yellow bracket). **c**, Space filling model viewed from the bare zone (compare with Figs 2a and 4b) showing S2's (red) making intramolecular contacts with the actin-binding region of the blocked motor domain (AB, left arrow) and intermolecular contacts with the converter (Cnv) and SH3 regions of the blocked motor domain (right arrow).

activity by phosphorylation of the regulatory light chains^{24–26}. This breaks the bonds attaching the heads to each other³ and to the filament surface, such that they become mobile and disordered^{26,27}. They now act independently of each other, and are free to interact with actin, leading to contraction

A striking and unexpected revelation from our studies is the finding that the atomic structure of a vertebrate smooth muscle myosin molecule gives an excellent fit to the EM reconstruction of an invertebrate striated muscle myosin filament. The precision of this fit between such distantly related systems suggests that the intramolecular, interacting-head structure may be a general motif for the relaxed state of phosphorylation-regulated myosin filaments in smooth and striated muscles of many species^{24–26} (although the intermolecular interactions may vary). Evidence that this structure may also occur in filaments regulated by direct Ca^{2+} binding comes from EM of scallop myosin molecules, where interacting heads¹⁹ (pointing back towards the tail^{19,20}) also characterize the OFF state. The similarity of nonmuscle myosin II to smooth muscle myosin suggests that nonmuscle myosin, although monomeric in the OFF-state²⁵, will also adopt this structure. The ordered heads of relaxed vertebrate striated muscle are apparently close to each other¹² and, like tarantula filaments²⁶, become disordered on phosphorylation, enhancing their activity²⁷. This suggests that comparable (possibly weaker) interactions could also hold the heads in place in the dephosphorylated state of vertebrate striated muscle. We are currently carrying out studies on thick filaments from other systems to test these possibilities.

METHODS

Preparation of tarantula thick filaments. Thick filaments from tarantula muscle were studied because they have a highly ordered array of heads⁷, whose activity is regulated by phosphorylation²⁶, similar to the closely related *Limulus*²⁴. Filaments were isolated from tarantula leg by homogenization of detergent skinned muscle in a relaxing medium, and purified free of thin filaments using gelsolin to sever actin²⁸.

Cryo-electron microscopy. Filaments were prepared for cryo-electron microscopy using holey carbon films glow-discharged in an atmosphere of amyamine. Blotting and freezing in liquid ethane were carried out in a humid chamber at 80% relative humidity²⁸. Micrographs for image processing were recorded on Kodak S0163 film under low dose conditions on a Philips CM120 cryo-electron microscope, using a defocus of $\sim 1.5 \mu\text{m}$.

Image processing. Negatives were scanned on an Agfa DuoScan T2000 XL at a pixel size of 0.53 nm in the original specimen. Filaments were aligned with the bare zone at the top before scanning, to ensure the correct polarity in subsequent steps. Reconstruction of helical objects, such as myosin filaments, is traditionally carried out by helical techniques, which take advantage of the fact that a single projection image contains many different views of the repeating subunit. When the symmetry of a filament involves a relatively small integer number of subunits per turn, as with many myosin filaments, this benefit is significantly reduced, and strictly helical approaches become more difficult⁷. We therefore carried out 3D reconstruction by the Iterative Helical Real Space Reconstruction (IHRSR) single particle method¹³, using the SPIDER software package²⁹, which avoids this limitation. The reconstruction was based on $\sim 5,000$ segments, each 53 nm long with an overlap of 48 nm, from ~ 60 different filament halves. The total number of unique pairs of myosin heads that went into the reconstruction was $\sim 7,200$. Initial reference models used for the reconstruction were helical reconstructions derived either from an earlier negative stain data set⁷ or the current cryo data. All gave the same final structure. The resolution of the reconstruction was ~ 2.5 nm according to Fourier shell correlation (FSC) using a 0.5 threshold. Accordingly, the reconstruction was low pass filtered to 2.5 nm. Surface renderings were carried out with UCSF Chimera³⁰. Computational fitting of the atomic model of smooth muscle HMM (PDB 1i84) (ref. 3) to the reconstruction was carried out manually within Chimera.

Received 2 March; accepted 13 June 2005.

1. Geeves, M. A. & Holmes, K. C. Structural mechanism of muscle contraction. *Annu. Rev. Biochem.* **68**, 687–728 (1999).
2. Lehman, W. & Szent-Györgyi, A. G. Regulation of muscular contraction. Distribution of actin control and myosin control in the animal kingdom. *J. Gen. Physiol.* **66**, 1–30 (1975).
3. Wendt, T., Taylor, D., Trybus, K. M. & Taylor, K. Three-dimensional image reconstruction of dephosphorylated smooth muscle heavy meromyosin reveals

- asymmetry in the interaction between myosin heads and placement of subfragment 2. *Proc. Natl Acad. Sci. USA* **98**, 4361–4366 (2001).
4. Craig, R. & Padrón, R. in *Myology* (eds Engel, A. G. & Franzini-Armstrong, C.) 129–166 (McGraw-Hill, New York, 2004).
 5. Huxley, H. E. & Brown, W. The low-angle x-ray diagram of vertebrate striated muscle and its behaviour during contraction and rigor. *J. Mol. Biol.* **30**, 383–434 (1967).
 6. Wray, J. S., Vibert, P. J. & Cohen, C. Diversity of cross-bridge configurations in invertebrate muscles. *Nature* **257**, 561–564 (1975).
 7. Crowther, R. A., Padrón, R. & Craig, R. Arrangement of the heads of myosin in relaxed thick filaments from tarantula muscle. *J. Mol. Biol.* **184**, 429–439 (1985).
 8. Offer, G., Knight, P. J., Burgess, S. A., Alamo, L. & Padrón, R. A new model for the surface arrangement of myosin molecules in tarantula thick filaments. *J. Mol. Biol.* **298**, 239–260 (2000).
 9. Stewart, M., Kensler, R. W. & Levine, R. J. Three-dimensional reconstruction of thick filaments from *Limulus* and scorpion muscle. *J. Cell Biol.* **101**, 402–411 (1985).
 10. Stewart, M. & Kensler, R. W. Arrangement of myosin heads in relaxed thick filaments from frog skeletal muscle. *J. Mol. Biol.* **192**, 831–851 (1986).
 11. Vibert, P. Helical reconstruction of frozen-hydrated scallop myosin filaments. *J. Mol. Biol.* **223**, 661–671 (1992).
 12. Eakins, F., AL-Khayat, H. A., Kensler, R. W., Morris, E. P. & Squire, J. M. 3D Structure of fish muscle myosin filaments. *J. Struct. Biol.* **137**, 154–163 (2002).
 13. Egelman, E. H. A robust algorithm for the reconstruction of helical filaments using single-particle methods. *Ultramicroscopy* **85**, 225–234 (2000).
 14. Wray, J. S. Structure of the backbone in myosin filaments of muscle. *Nature* **277**, 37–40 (1979).
 15. Liu, J., Wendt, T., Taylor, D. & Taylor, K. Refined model of the 10S conformation of smooth muscle myosin by cryo-electron microscopy 3D image reconstruction. *J. Mol. Biol.* **329**, 963–972 (2003).
 16. Burgess, S. A., Walker, M. L., White, H. D. & Trinick, J. Flexibility within myosin heads revealed by negative stain and single-particle analysis. *J. Cell Biol.* **139**, 675–681 (1997).
 17. Suzuki, H., Stafford, W. F. III, Slayter, H. S. & Seidel, J. C. A conformational transition in gizzard heavy meromyosin involving the head-tail junction, resulting in changes in sedimentation coefficient, ATPase activity, and orientation of heads. *J. Biol. Chem.* **260**, 14810–14817 (1985).
 18. Burgess, S. A. *et al.* Structure of smooth muscle myosin in the switched-off state. *Biophys. J.* **82**, 356a (2002).
 19. Jung, H. *et al.* Comparative studies of the folded structures of scallop striated and vertebrate smooth muscle myosins. *Biophys. J.* **86**, 403a (2004).
 20. Stafford, W. F. *et al.* Calcium-dependent structural changes in scallop heavy meromyosin. *J. Mol. Biol.* **307**, 137–147 (2001).
 21. Trybus, K. M., Freyzon, Y., Faust, L. Z. & Sweeney, H. L. Spare the rod, spoil the regulation: necessity for a myosin rod. *Proc. Natl Acad. Sci. USA* **94**, 48–52 (1997).
 22. Rovner, A. S. A long, weakly charged actin-binding loop is required for phosphorylation-dependent regulation of smooth muscle myosin. *J. Biol. Chem.* **273**, 27939–27944 (1998).
 23. Trybus, K. M., Naroditskaya, V. & Sweeney, H. L. The light chain-binding domain of the smooth muscle myosin heavy chain is not the only determinant of regulation. *J. Biol. Chem.* **273**, 18423–18428 (1998).
 24. Sellers, J. R. Phosphorylation-dependent regulation of *Limulus* myosin. *J. Biol. Chem.* **256**, 9274–9278 (1981).
 25. Sellers, J. R. Regulation of cytoplasmic and smooth muscle myosin. *Curr. Opin. Cell Biol.* **3**, 98–104 (1991).
 26. Craig, R., Padrón, R. & Kendrick-Jones, J. Structural changes accompanying phosphorylation of tarantula muscle myosin filaments. *J. Cell Biol.* **105**, 1319–1327 (1987).
 27. Levine, R. J., Kensler, R. W., Yang, Z., Stull, J. T. & Sweeney, H. L. Myosin light chain phosphorylation affects the structure of rabbit skeletal muscle thick filaments. *Biophys. J.* **71**, 898–907 (1996).
 28. Hidalgo, C., Padrón, R., Horowitz, R., Zhao, F. Q. & Craig, R. Purification of native myosin filaments from muscle. *Biophys. J.* **81**, 2817–2826 (2001).
 29. Frank, J. *et al.* SPIDER and WEB: processing and visualization of images in 3D electron microscopy and related fields. *J. Struct. Biol.* **116**, 190–199 (1996).
 30. Pettersen, E. F. *et al.* UCSF Chimera—a visualization system for exploratory research and analysis. *J. Comput. Chem.* **25**, 1605–1612 (2004).

Supplementary Information is linked to the online version of the paper at www.nature.com/nature.

Acknowledgements We thank R. Horowitz, W. Lehman and A. Pirani for their help in this work. Support was provided by grants from the National Institutes of Health to R.C. and to E.H.E., an International Research Scholar grant from the Howard Hughes Medical Institute to R.P. and a grant from the National Fund for Science, Technology and Innovation (FONACIT, MCT) to R.P. Electron microscopy was carried out in the Core Electron Microscopy Facility of the University of Massachusetts Medical School, supported in part by grants from the NIH. Molecular graphics images were produced using the UCSF Chimera package from the Computer Graphics Laboratory, University of California, San Francisco, supported by a grant from the NIH.

Author Information Reprints and permissions information is available at npg.nature.com/reprintsandpermissions. The authors declare no competing financial interests. Correspondence and requests for materials should be addressed to R.C. (Roger.Craig@umassmed.edu).